Environ Earth Sci (2013) 68:1527–1538
DOI 10.1007/s12665-012-1846-1

ORIGINAL ARTICLE

# Multivariate statistical analysis and 3D-coupled Markov chain modeling approach for the prediction of subsurface heterogeneity of contaminated soil management in abandoned Guryong Mine Tailings, Korea

**Yonghee Moon · Yong-Seon Zhang · Yungoo Song · Eungyu Park · Hi-Soo Moon**

Received: 15 February 2011 / Accepted: 9 July 2012 / Published online: 24 July 2012
© Springer-Verlag 2012

**Abstract** Various geological materials on the ground surface can be natural or artificial sources of pollutions. The spatial distribution of tailings is required to investigate the geological material pollutions. The objectives of this study were to determine the main factors influencing tailing zonations using a factor analysis, to determine the zonation of tailings with a cluster analysis, and to simulate zonations with three-dimensional coupled Markov chain (3D-CMC) modeling. The database was composed of 12 excavated exploratory holes in the Guryong mine tailings, for which there were analytical data covering the physical, chemical, and mineralogical aspects. The principal component analysis indicated that the tailing composition was mainly affected by three factors out of 21 variables: pH, cation exchange capacity, and mineral composition. Based on these main factors, the tailings were classified into five groups using a cluster analysis. Group I was approximately 50 cm deep from surface and had secondary gypsum ($CaSO_4{\cdot}2H_2O$) and jarosite ($KFe_3(SO_4)_2(OH)_6$). Group II had low pH values caused by strong pyrite oxidation and the greatest amounts of the secondary minerals. In group III and IV, the quantity of the secondary minerals decreased. Group V was characterized by primary calcite ($CaCO_3$) composition. These results were applied to the CMC modeling, and the quantitative 3D distribution of tailing was verified. For the cost-saving prediction of subsurface heterogeneity, 3D-CMC modeling was executed using the selected eight holes data among twelve holes. The unknown four holes, GS3, GS6, GS8 and GS11, are identified as 89.7, 88.6, 80.7 and 81.1 %, respectively. They are recognized as 85.0 % of the total zonation. The zonation method of tailings executed in this study can be utilized in predicting the 3D distribution of the pollution factor. This may be a useful and economical method to identify the environmentally hazardous materials in underground systems.

**Keywords** Principal component analysis · Cluster analysis · Pyrite · Gypsum · Jarosite

Y. Moon · Y.-S. Zhang
National Institute of Agricultural Science and Technology, Su-won 441-707, Korea
e-mail: yhmoon9@korea.kr

Y. Song (✉) · H.-S. Moon
Department of Earth System Sciences, Yonsei University, Seoul 120-749, South Korea
e-mail: yungoo@yonsei.ac.kr

E. Park
Department of Geology, Kyungpook National University, Daegu 702-701, Korea

## Introduction

The sulfide-rich tailings are a potential source of low-pH condition that results from the oxidation of sulfide minerals, such as pyrite ($FeS_2$). The degree of sulfide alteration can be expressed with an index value from 0 to 10 with 0, representing no alteration and 10 representing complete alteration of the tailings as a whole, and the oxidation profiles are divided into the three zones (Blowes and Jambor 1990). Multivariate statistical analysis is a mathematical technique applied in multiple fields of geological investigations, such as geochemistry (Häkli 1970), petrography (Saager and Esselaar 1969), hydrogeology (Kim et al. 2005; Lambrakis et al. 2004), and environmental geology (Davis 1986; Grande et al. 1996). Acosta et al. (2011) and Hwang et al. (2001) present the spatial variations using the multivariate statistical approach in the mine area, but do not incorporate uncertainty in the spatial prediction. Uncertainties in spatial

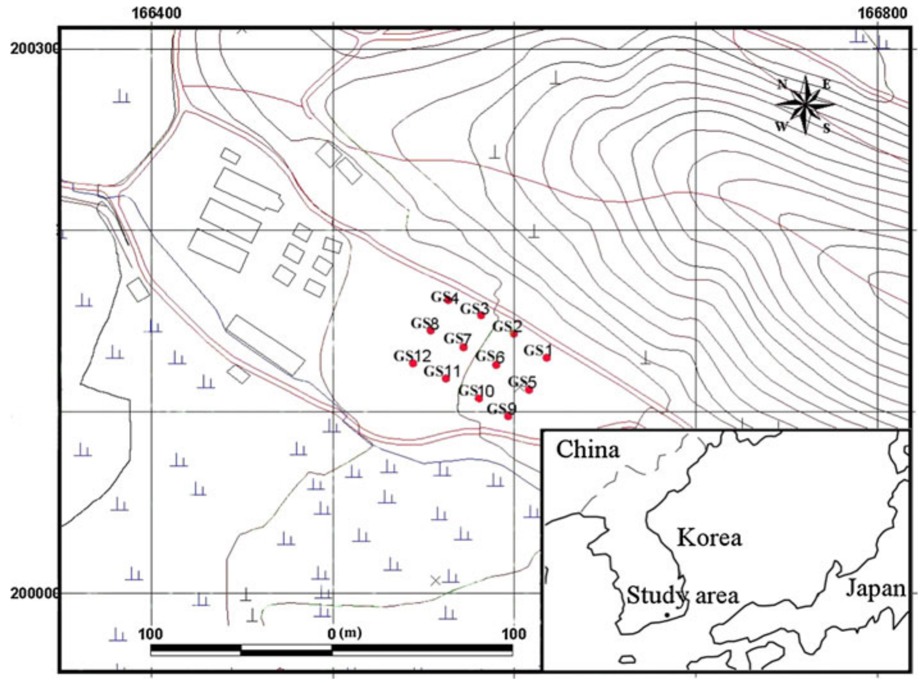


**Fig. 1** The map showing the sample location of tailing in the Guryong mine located 50 km northeast of Changwon, Korea. The *12 circles* are sampling point

predictions give rise to considerable uncertainty in applications such as risk assessment, cost estimation, and decision analysis (Li 2006; Li and Zhang 2005). Carle and Fogg (1996, 1997) introduced the Markov chain based on indicator geostatistics, where the variograms conventionally used by geostatisticans are substituted by Makovian transitions. Park et al. (2005) improved two-dimensional coupled Markov chain (CMC) model by applying the model to sparsely distributed data directly stemming from the work of Elfeki and Dekking (2001). They also demonstrated the validity of the CMC in the three-dimensional space. For the estimation of the spatial distribution of each horizon, the three-dimensional CMC modeling was applied (Park et al. 2005; Park 2010).

This study aimed to provide specific information regarding the mineralogical and physico-chemical characterization and interactions that occur horizontally and vertically within tailings in the Guryong mine, where the abundant sulfide mineral is pyrite. From the results of this study, the entire profile could suggest zonation and verify the multivariate statistic analysis and 3D CMC modeling as useful methods for determining the spatial distribution of the tailings.

## Description of the studied tailing area

The Guryong mine copper deposit was located in Buk-myeon, Changwon City, South Korea (128°38′00″–128°38′30″E, 35°17′30″–35°18′00″N; Fig. 1). The area around the Guryong mine was underlain by andesite, which was the host rock of the Cu-deposit. The deposits were composed of many sulfide veins and of altered zones that may be the result of hydrothermal solutions. The Cu ore is typically composed of alternating bands of pyrite, chalcopyrite, calcite and quartz, and their bands were widely distributed within the deposits (Kim and Oh 1966). The principal gangue minerals were silicates such as quartz, chlorite, mica and feldspar. The major steps in the milling process were grinding, aeration and flotation. The tailings impoundment, which operated from 1945 to 1971, has a surface area of approximately 40,000 $m^2$. The tailings were deposited at 200–700 cm depth, which was immediately above the bedrock. The runoff generated from the impoundment ran into small streams that ended at nearby farmland (Min et al. 1998). The average annual precipitation was 1,509 mm and fell mainly during the summer. The depths of the saturation zone below the tailings surface varied; however, the average depth was less than 250 cm below the surface. The hydraulic conductivity of the tailings ranged from $8.7 \times 10^{-5}$ cm/s to $1.6 \times 10^{-2}$ cm/s. The saturation originated from a perched aquifer in the mine tailings. The porosity values ranged between 0.25 and 0.56 (Moon 2007).

## Materials and methods

### Sampling methods

The sampling site was constructed as elemental data using GPS (Fig. 1, $60 \times 40 \times 10$ m). Percussion drilling equipment was used to reach depths of 10 m in the first field sampling expedition in 2004, during which twelve holes were drilled. However, the GS1, GS2, GS3, and GS4 holes are drilled to only 7 m. The cores for analysis were collected in sections 1 m long and approximately 4 cm in diameter. Each meter of drill core was separated into five 20 cm lengths. Smaller sub-samples were taken, when colors change. Twelve holes were drilled in the tailings, from which 364 samples were collected. The samples were sealed in plastic bottles and stored in an ice-packed cooler box until ready for study.

### Experimental methods

The samples were air-dried (25 °C) and sieved to 2 mm in the laboratory. The dry samples were stored in polyethylene containers at room temperature. Each sample was analyzed for its physical (particle distribution), chemical (acid-leachable fraction and cation exchange capacity) and mineralogical characteristics. The particle size distributions of all samples were measured by a grain-size analyzer (Mastersizer 2000, Malvern Instruments Ltd). The analyzer separated each sample into clay (<2 μm), silt (2–53 μm) and sand (>53 μm) fractions. The cation exchange capacity (CEC) was measured following the work of Borden and Giese (2001). The pH was determined in a 1:5 ratio suspension of dewatered tailings using a 6107BN, Thermo Orion pH meter, according to the international standard. The acid-leachable fraction was determined by dissolving a 5.0 g sample of dried tailings in 50 ml of 20 % (v/v) HCl for 1 h in a 30 °C water bath. The acidified water samples were analyzed by spectrophotometer (HACH DR/4000U) for Al, Fe, Mn, and Cu, and by ICP-Mass (Perkin Elmer ELAN 6100) for Pb, Zn and Cd. All of the samples were analyzed as a bulk sample by X-ray diffraction (XRD), using a Max-Science MXP-3 system. The quantitative analysis of the minerals was performed with the SIROQUANT V2.5 program (Taylor and Zhu 1992).

## Multivariate statistical analysis and geostatic approach

### Principal component analysis

Factor analysis, including principal component analysis (PCA) was carried out to reveal the interaction among the variables. The PCA is a multivariate statistical technique used for data reduction and for deciphering patterns within large sets of data (Wold 1987; Joliffe 1986). The principal components are calculated so that they take into account the correlations present in the original data, but are uncorrelated to one another. Generally, the first two or three principal components account for the majority of the variance in the original data, thus reducing the data to two or three dimensions. The goal of the PCA is to describe the majority of the variance in the large dataset in a few principal components, with the remaining unexplained variance consisting of nose (Gauch 1993).

### Cluster analysis

The cluster analysis (CA) was applied to the factor scores obtained from the factor analysis, to separate the tailing samples into several physical, chemical and mineralogical regimes. The CA refers to a set of techniques designed to classify observations; therefore, members of the resulting groups are similar to each other but distinct from other groups. Hierarchical clustering, which successively joins the most similar observations, is one of the most common approaches (Davis 1986). However, the CA applied in this study was the nonhierarchical type. This type has been applied to *K*-means method for sample classification. A set of K seed points can be used as cluster nuclei around which the set of *m* data units can be grouped. The following methods are representative examples of how such seed point can be generated (Anderberg 1973).

### Coupled Markov chain model

The coupled Markov chain (CMC) in two-dimensional space has been described by Elfeki and Dekking (2001). In the Markovian framework, the conditional distribution of any future state is independent of the past history if the present state is given. That is, if the discrete stochastic process {Zn, $n = 0, 1, 2, \ldots$} is a sequence of random variables taking values in the state space{$S1, S2, \ldots, Sn$} (Fig. 2), then the sequence is a Markovian process if (Ross 2000):

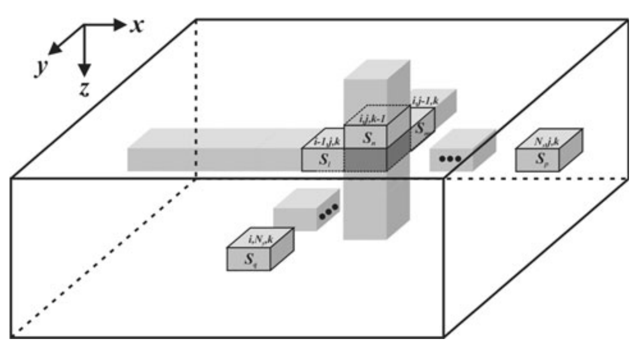


**Fig. 2** Schematic diagram of one-dimensional coupled Markov chain calculation ($S_p$, state of cell *M*; $S_j$, state of cell *l*; and *Sq*, state of cell *N*; Park et al. 2005)

$$\Pr(Z_i = S_k/Z_{i-l} = S_l, Z_{i-2} = S_n, Z_{i-3} = S_r, \ldots, Z_0 = S_p) \\ = \Pr(Z_i = S_k/Z_{i-l} = S_l) = P_{lk} \quad (1)$$

where $P_{lk}$ is the transition probability from a state ($S_l$) to another state ($S_k$). Transition probabilities can be estimated from the relative frequencies of transitions from a certain state to other states. These transition probabilities can be arranged into an $n \times n$ matrix:

$$P = \begin{vmatrix} P_{11} & \cdot & \cdot & \cdot & P_{1n} \\ \cdot & \cdot & \cdot & \cdot & \cdot \\ \cdot & \cdot & P_{1k} & \cdot & \cdot \\ \cdot & \cdot & \cdot & \cdot & \cdot \\ P_{11} & \cdot & \cdot & \cdot & P_{nn} \end{vmatrix} \quad (2)$$

where $n$ is the number of states in the system. In the matrix $P$, all elements must be non-negative ($P_{1k} \geq 0$), and the sum of the elements in each row is shown in Eq. 1. The transition probabilities considered in Eq. 2 are called one-step transition, meaning that the transition from one state to another occurs in one step.

The conditional probability equation that is governed by the immediate past and the future state was derived by Elfeki and Dekking (2001):

$$\Pr(Z_i = S_k/Z_{i-l} = S_l, Z_N = S_q) = \frac{p_{jq}^{N-i} P_{lj}}{p_{lq}^{N-i+1}} \quad (3)$$

where $Z_N$ is a random variable of the future, and $S_q$ is the future state.

This can be extended to three-dimensional space by coupling three state spaces, $\{S_1,S_2, \ldots, S_n\} \times \{S_1,S_2, \ldots, S_n\} \times \{S_1,S_2, \ldots, S_n\}$, with the assumption that a transition to a given location in three-dimensional space from two independent chains must be to the same state from both chains (Fig. 2). A simple modification to Eq. (3) yields the three-dimensional CMC formulation (Park 2010). The algorithm for stochastic prediction was examined following the steps described by Park (2010).

## Results and discussion

### Physico-chemical and mineralogical characteristic of tailing

The representative drill core investigation of this study indicated that the tailings were underlain by 200–700 cm of soil over bedrock. The physico-chemical and mineral quantitative analysis of the representatives collected from the GS3, GS6 and GS12 core samples in the Guryong mine tailings are presented in Table 1 and Fig. 3, and the others are presented in Moon (2007). The presented sampling points are not adjoining to each row a representative (Fig. 1).

The pH values of the samples ranged between 3.0 and 8.0. In the shallow tailings, the pH was less than 3.3, but it increased with depth to greater than pH 7.0, suggesting that the acidic pore water was being neutralized (Fig. 3). Except for the GS3 core, which lacked a water table, the GS12 drill core containing fine tailing particles near the water table (approximately 250 cm) was confirmed calcite ($CaCO_3$), which can neutralize acid. However, the GS6 cores contained coarse particles near the water table, did not have observed calcite (Table 1) and did not increase to a pH greater than pH 6.0 (Fig. 3). The tailing grain size and moisture content were associated with the sulfide mineral oxidation (Blowes and Jambor 1990; Moon et al. 2008a). In this study area, the most abundant sulfide mineral was pyrite which oxidizes readily when exposed to water and atmospheric oxygen. The oxidation of sulfide minerals was evident by the yellowish brown color (10YR 5/6) of the surficial tailings compared to the dark grey color (N6/0) of the tailings (Table 1).

The $Fe^{2+}$ generated by pyrite oxidation may be further oxidized, hydrolyzed and precipitated as jarosite, schwertmannite and Fe-oxyhydroxide which have confirmed the presence by SEM–EDX (Fig. 4) in the work of Moon et al. (2008b). This suggested the proposed schematic model for mineral cycling in the tailings (Fig. 5), which can be found when the dissolution of primary and precipitated secondary minerals had generated a low-pH condition by oxidizing pyrite. Figure 5 can be summarized that the oxidation of pyrite is the most important reaction controlling the changes in pH, the dissolution of the primary silicates and carbonates, the precipitation of secondary mineral phases, acid neutralizing, and heavy metal behaviors through the profile.

An extensive investigation of the sulfide mineral oxidation mechanisms has been presented by Nordstrom (1982), Blowes and Jambor (1990), and McGregor et al. (1998). The evidence of sulfide-oxidation reactions in the tailings are the depletion of sulfide minerals in the near sub-surface zone of the tailings. The XRD patterns for a representative sample of the tailings (GS6 and GS12) exhibited large differences in mineralogy that changed markedly with depth (Table 1). The mineralogical and major ion analysis of the tailing solids conducted in conjunction with the detailed pore water analysis provided greater insight into the future geochemistry evolution (Blowes et al. 1998). The analyses for major ions and acid-leachable fraction were performed on samples of tailing solids collected below the tailings surface. The concentration of the acid-leachable fraction and whole rock analyses of tailings was similar to those from observation (Fig. 3). The results of the acid–base accounting were

**Table 1** Physical properties and mineral quantitative analysis of the collected samples from the representative GS3, GS6 and GS12 cores in the Guryong mine tailings

| | Depth (cm) | Wet color | Size fraction (vol. %, <2 mm) | | | Mineral composition (wt. %) | | | | |
|---|---|---|---|---|---|---|---|---|---|---|
| | | | Clay | Silt | Sand | Py | Chl | Gy | Ja | Calc |
| GS3 | | | | | | | | | | |
| 1 | 0–45 | 7.5YR4/3 | 10.4 | 45.0 | 44.6 | 0.0 | 11.5 | 4.4 | 0.0 | 0.0 |
| 2 | 45–50 | 2.5Y5/2 | 10.1 | 38.7 | 51.2 | 0.0 | 7.5 | 3.2 | 0.0 | 0.0 |
| 3 | 50–60 | 2.5GY6/1 | 11.9 | 70.9 | 17.2 | 14.1 | 3.3 | 17.8 | 0.0 | 0.0 |
| 4 | 60–80 | 7.5Y4/2 | 8.3 | 53.5 | 38.2 | 24.0 | 11.8 | 14.3 | 0.0 | 0.0 |
| 5 | 80–100 | 10Y4/1 | 16.4 | 82.1 | 1.5 | 20.9 | 16.0 | 8.9 | 0.2 | 0.0 |
| 6 | 100–155 | 5GY3/1 | 0.9 | 15.3 | 83.8 | 17.1 | 21.8 | 3.9 | 0.0 | 0.0 |
| 7 | 155–172 | 2.5Y4/4 | 0.9 | 12.1 | 87.0 | 3.4 | 26.8 | 8.7 | 0.0 | 0.0 |
| 8 | 172–200 | 7.5Y4/2 | 3.9 | 34.0 | 62.1 | 19.0 | 22.9 | 7.9 | 0.0 | 0.0 |
| 9 | 200–250 | 10Y3/2 | 1.4 | 14.3 | 84.3 | 19.2 | 17.4 | 15.9 | 0.0 | 0.0 |
| 10 | 250–270 | 10YR3/4 | 4.0 | 30.9 | 65.1 | 27.2 | 20.4 | 12.5 | 0.0 | 0.0 |
| 11 | 270–280 | 2.5GY4/1 | 4.8 | 30.7 | 64.5 | 10.3 | 26.0 | 15.3 | 0.0 | 0.0 |
| 12 | 280–300 | 10Y4/2 | 5.4 | 43.8 | 50.8 | 19.6 | 29.4 | 19.7 | 0.0 | 0.0 |
| GS6 | | | | | | | | | | |
| 1 | 0–25 | 10YR4/2 | 20.3 | 65.8 | 13.9 | 0.0 | 8.5 | 0.0 | 7.5 | 0.0 |
| 2 | 25–40 | 2.5Y6/4 | 8.3 | 21.3 | 70.4 | 0.0 | 5.1 | 4.0 | 18.3 | 0.0 |
| 3 | 40–60 | 10Y4/4 | 4.2 | 29.0 | 66.8 | 48.7 | 9.7 | 3.8 | 0.0 | 0.0 |
| 4 | 60–75 | G4/1 | 0.7 | 10.1 | 89.2 | 39.8 | 9.5 | 3.5 | 0.0 | 0.0 |
| 5 | 75–100 | N3/0 | 1.4 | 19.5 | 79.1 | 36.6 | 13.2 | 3.9 | 0.0 | 0.0 |
| 6 | 100–160 | 7.5GY4/1 | 0.5 | 6.9 | 92.6 | 58.4 | 9.8 | 1.4 | 0.0 | 0.0 |
| 7 | 160–180 | GY4/1 | 0.5 | 8.1 | 91.3 | 52.3 | 13.1 | 3.7 | 0.0 | 0.0 |
| 8 | 180–185 | 10GY4/1 | 1.9 | 18.1 | 80.0 | 33.4 | 16.1 | 9.4 | 1.7 | 0.0 |
| 9 | 185–200 | 5Y4/1 | 6.1 | 52.1 | 41.8 | 18.5 | 23.4 | 14.9 | 1.2 | 0.0 |
| 10 | 200–280 | GY4/1 | 3.6 | 23.5 | 72.9 | 20.3 | 23.2 | 9.0 | 0.9 | 0.0 |
| 11 | 280–300 | 2.5GY4/1 | 9.8 | 51.2 | 39.0 | 30.3 | 24.6 | 6.1 | 2.1 | 0.0 |
| 12 | 300–400 | G4/1 | 3.9 | 20.3 | 75.8 | 20.7 | 22.3 | 7.3 | 0.5 | 0.0 |
| 13 | 400–450 | 7.5GY4/1 | 2.9 | 17.0 | 80.1 | 31.2 | 23.5 | 10.9 | 0.2 | 0.0 |
| 14 | 450–470 | N4/0 | 7.0 | 38.2 | 54.8 | 11.1 | 33.8 | 4.8 | 0.0 | 0.0 |
| 15 | 470–475 | 2.5GY3/1 | 10.7 | 53.9 | 35.4 | 6.2 | 14.9 | 2.5 | 1.0 | 0.0 |
| 16 | 475–500 | 10YR3/2 | 15.9 | 59.1 | 25.0 | 1.7 | 5.1 | 3.5 | 0.6 | 0.0 |
| 17 | 500–555 | 7.5YR3/4 | 19.7 | 55.0 | 25.3 | 0.0 | 5.8 | 3.0 | 0.0 | 0.0 |
| 18 | 570–570 | 10YR4/3 | 16.5 | 42.3 | 41.2 | 0.0 | 6.9 | 2.7 | 0.0 | 0.0 |
| 19 | 570–600 | 10YR4/3 | 10.2 | 31.1 | 58.7 | 0.0 | 19.0 | 1.7 | 0.0 | 0.0 |
| GS12 | | | | | | | | | | |
| 1 | 0–62 | 2.5YR3/4 | 18.4 | 64.9 | 16.7 | 0.0 | 10.7 | 1.6 | 0.0 | 0.0 |
| 2 | 62–75 | 10YR4/5 | 15.8 | 67.7 | 16.5 | 0.0 | 18.5 | 2.5 | 5.1 | 0.0 |
| 3 | 75–80 | 5YR3/4 | 18.9 | 65.6 | 15.6 | 0.0 | 13.9 | 11.5 | 3.0 | 0.0 |
| 4 | 80–100 | 7.5YR4/3 | 20.3 | 64.8 | 14.9 | 1.0 | 12.4 | 15.4 | 4.0 | 0.0 |
| 5 | 100–170 | 5Y3/2 | 16.2 | 72.0 | 11.8 | 22.5 | 16.6 | 9.7 | 0.9 | 0.0 |
| 6 | 170–175 | N4/0 | 1.8 | 31.9 | 66.3 | 16.3 | 11.6 | 10.9 | 0.0 | 0.0 |
| 7 | 175–180 | 7.5Y4/2 | 2.3 | 24.5 | 73.2 | 9.7 | 15.3 | 11.7 | 0.0 | 0.0 |
| 8 | 180–185 | 7.5Y4/2 | 1.9 | 18.6 | 79.5 | 8.7 | 12.8 | 10.3 | 0.0 | 0.0 |
| 9 | 185–200 | 2.5Y3/2 | 2.7 | 18.7 | 78.6 | 5.0 | 13.4 | 8.5 | 0.0 | 0.0 |
| 10 | 200–230 | 10GY4/1 | 6.9 | 42.9 | 50.2 | 11.5 | 19.4 | 11.3 | 0.0 | 0.0 |
| 11 | 230–250 | 10GY4/1 | 3.3 | 18.6 | 78.1 | 19.1 | 23.6 | 11.4 | 0.0 | 0.0 |
| 12 | 250–270 | N4/0 | 10.3 | 77.6 | 12.1 | 19.8 | 23.5 | 14.6 | 0.0 | 0.0 |

**Table 1** continued

| | Depth (cm) | Wet color | Size fraction (vol. %, <2 mm) | | | Mineral composition (wt. %) | | | | |
|---|---|---|---|---|---|---|---|---|---|---|
| | | | Clay | Silt | Sand | Py | Chl | Gy | Ja | Calc |
| 13 | 270–300 | N4/0 | 13.1 | 80.4 | 6.5 | 15.7 | 30.3 | 1.7 | 0.0 | 0.0 |
| 14 | 300–470 | 5G3/1 | 2.9 | 33.6 | 63.5 | 30.7 | 25.6 | 1.3 | 0.0 | 0.0 |
| 15 | 470–500 | N4/0 | 15.3 | 84.6 | 0.1 | 8.9 | 45.1 | 0.0 | 0.0 | 6.4 |
| 16 | 500–530 | 7.5Y5/1 | 13.8 | 84.0 | 2.2 | 8.8 | 51.7 | 0.0 | 0.0 | 4.3 |
| 17 | 530–550 | N4/0 | 14.1 | 85.9 | 0.0 | 9.3 | 51.2 | 0.0 | 0.0 | 4.4 |
| 18 | 550–570 | N4/0 | 18.2 | 81.8 | 0.0 | 11.0 | 38.0 | 0.0 | 0.0 | 4.9 |
| 19 | 570–600 | N4/0 | 19.2 | 80.8 | 0.0 | 8.3 | 33.2 | 0.0 | 0.0 | 4.0 |
| 20 | 600–675 | N3/0 | 7.1 | 42.9 | 50.0 | 0.3 | 5.9 | 1.1 | 0.0 | 0.0 |
| 21 | 675–680 | 10YR4/4 | 9.1 | 61.7 | 29.2 | 0.0 | 1.5 | 0.4 | 0.0 | 0.0 |
| 22 | 680–700 | 7.5YR3/3 | 2.5 | 21.5 | 76.0 | 0.0 | 1.5 | 0.0 | 0.0 | 0.0 |

*Py* pyrite, *Chl* chlorite, *Gy* gypsum, *Ja* jarosite, *Cal* calcite

analyzed to allow a more detailed prediction of the acid-producing potential of the tailings (Moon et al. 2008a). The results of this analysis showed a potential for acid generation in most samples, with the exception of those from surficial tailings. The potential for a given rock to generate and neutralize acid depends on its quantitative mineralogical composition and its particle size. An analysis of the chemistry of the major ions and a direct mineralogical quantitative analysis of bulk samples enables more detailed information on acid-neutralizing capacity. The $Fe_2O_3$ and $SO_3$ contents had few variations in the upper layer of tailings, which suggest the existence of jarosite, schwertmannite and Fe-oxyhydroxide as the secondary mineral phases (Moon et al. 2008b).

## Simplified parameters by PCA

Multivariate statistical analyses were performed with the physical (particle distribution), chemical (acid-leachable fraction and cation exchange capacity) and mineralogical data from Guryong mine tailing area, Korea. Multivariate statistical analyses were performed using a methodology suggested by Davis (1986). A statistical computer code was conducted with the well-known software package 'SPSS 12.0' (IBM Company).

Various physico-chemical and mineralogical results could be simplified using the PCA, which was applied to determine the interrelations among the 21 variables examined in the tailings. Accordingly, a small number of factors will usually account for approximately the same amount of information as do the much larger set of original variables (Lambrakis et al. 2004). There are many recommendations for selecting the optimal number of factor. According to this criterion, four factors have been chosen for this study. The factor analysis used in this study was the PCA with the practical application of varimax factor rotation (Kaiser 1958) for the reason that this method easily explains the PCA results. Generally, the first two or three principal components account for the majority of the original data, thus reducing the data to two or three dimensions (Gauch 1993). Table 2 provides the eigenvalues of the extracted factors, the eigenvalue differences among factors, and the proportions of total sample variance explained by the factors. The analysis generated 4 factors which accounted for 54.2 % of variance. The factors indicate communality. The bold numbers in Table 2 signify that the 21 variables belong anywhere in the factors. The first factor explained 19.3 % of the total variance, and demonstrated that most of the covariance in the system's properties may be explained by the variances of the cation exchange capacity (CEC), clay, silt, sand, albite and mica. The first factor emphasizes the principal role of clay, silt and sand in the physical composition of the tailings. The relationship among CEC, clay, silt and sand indicates influence on tailing weathering. The second, third and fourth factors explain 16.0, 9.5 and 9.4 % of the total variance, respectively, and 3.4, 2.0 and 2.0 of the eigenvalue, respectively. The second factor explained the relationship of the environment condition completed by the mineral dissolution. Most reactions in the gas, water and rock systems involve or are controlled by the pH of the system (Langmuir 1997). Other factors may express the relationship among pyrite oxidation, releasing $Fe^{2+}$ ions and precipitating a second mineral. The factor analysis indicates that tailing composition, which accounts for 54.2 % of the total variance in 21 variables, was mainly affected by three factors: pH, particle size and mineral composition (Table 2). The correlation between the PC1 and PC2 is given in Fig. 6. PC1 indicates the decrease of particle size and PC2 is related to the dissolution of minerals and the pH. These results might be related to the characteristics along the depth of the study area.

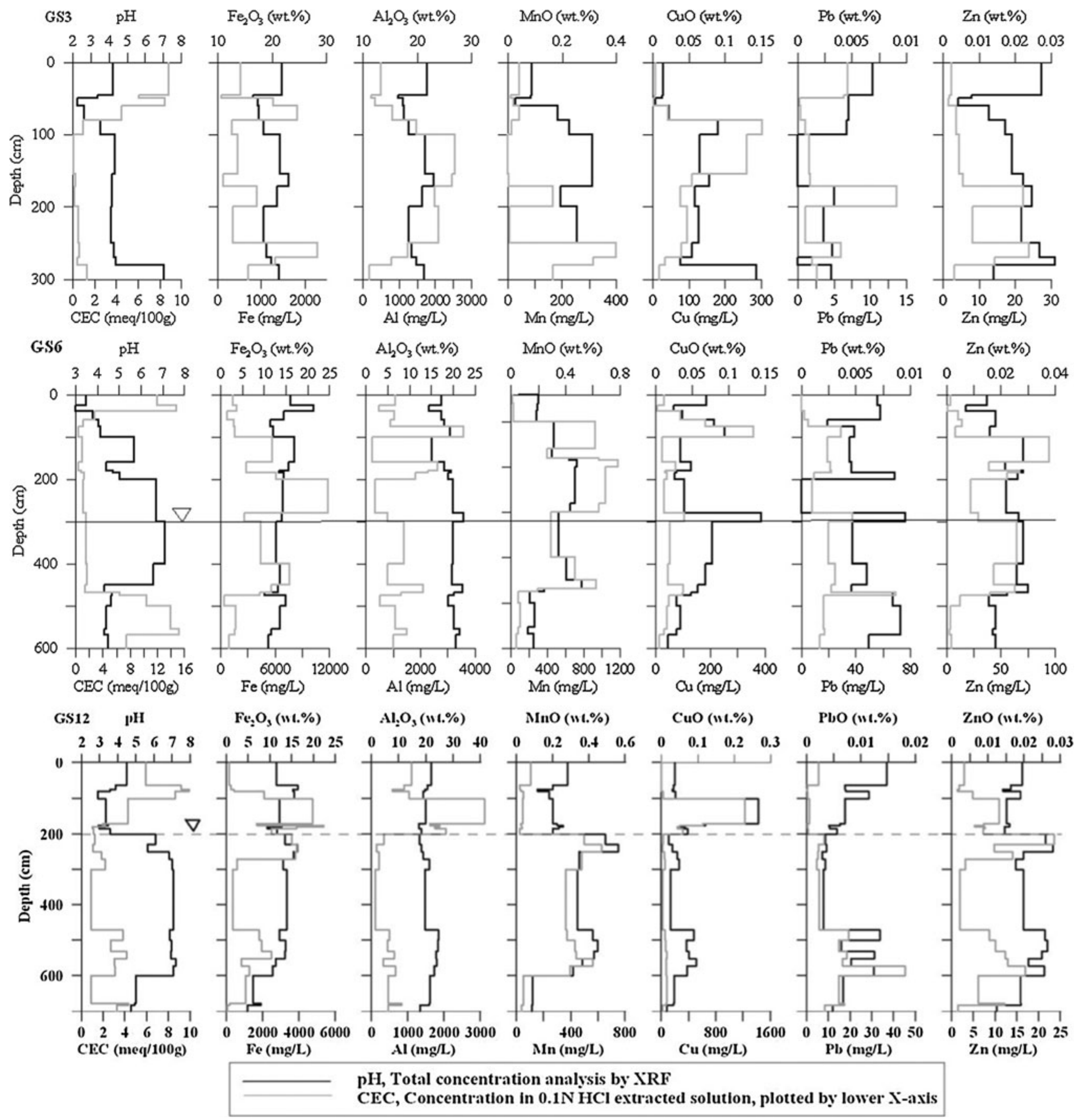


**Fig. 3** Diagrams showing the vertical changes in the total and 0.1 N HCl extracted of some representative elements for the core samples

## Zonation of tailings through cluster analysis

The 3D distribution of subsurface heterogeneity must be quantitatively characterized. The CA was performed based on the factor scores obtained from the factor analysis results. To suggest the zonations within tailings in this study, nonhierarchical CA has been applied to the *K*-means method for the sample classification. The *K*-means cluster analysis is an efficient tool for the zonation of the tailings, because it does not compute the distance between all pairs of cases (SPSS 2001). This method requires specifying the number of clusters. An initial cluster number of five zones was chosen that replicated the division of the tailings profile by Moon et al. (2008b). Table 3 presents an average value of variants for each group after cluster analysis for the 12-hole samples. The sand and silt among the parameters by the factor analysis were excluded from the cluster analysis, because these variables were affected by the

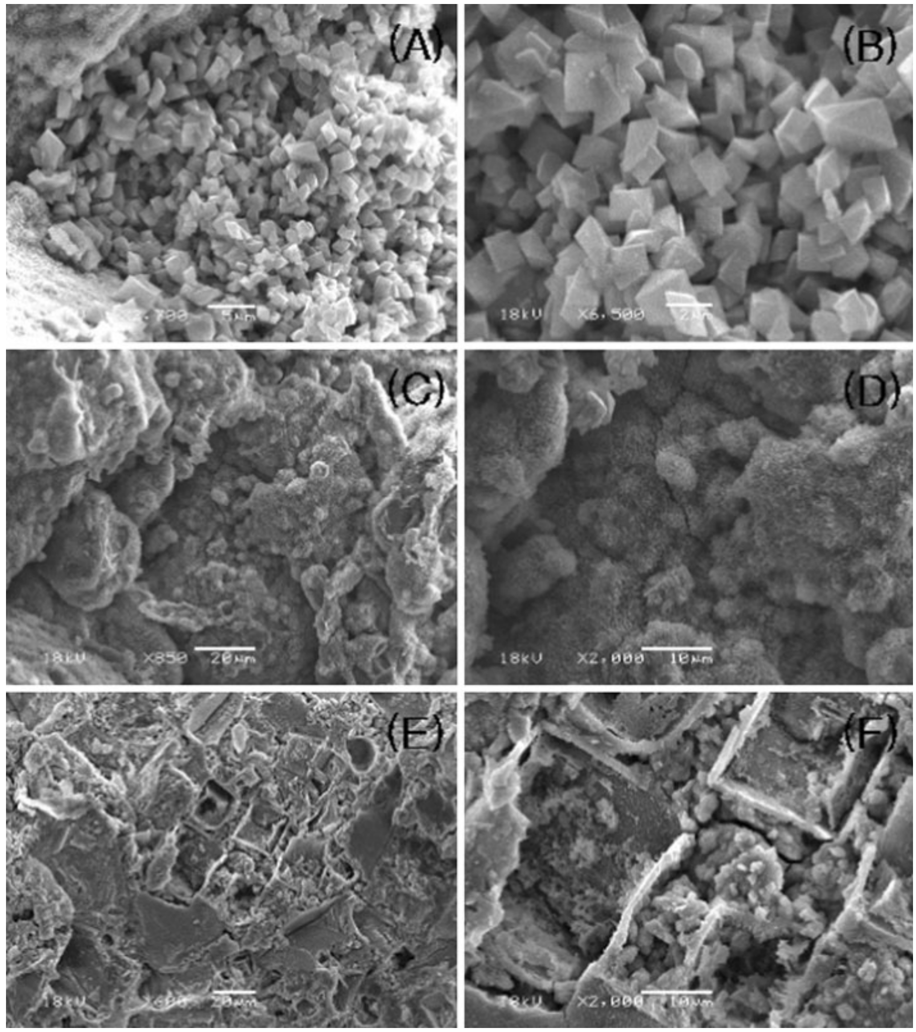


**Fig. 4** Scanning electron microscopic (SEM) images showing typical jarosite (**a**, **b**), schwertmannite (**c**, **d**), and Fe-oxyhyroxide [ferrihydrite, or amorphous $Fe(OH)_3$] (**e**, **f**) from the selected samples among core samples in Moon et al. (2008b)

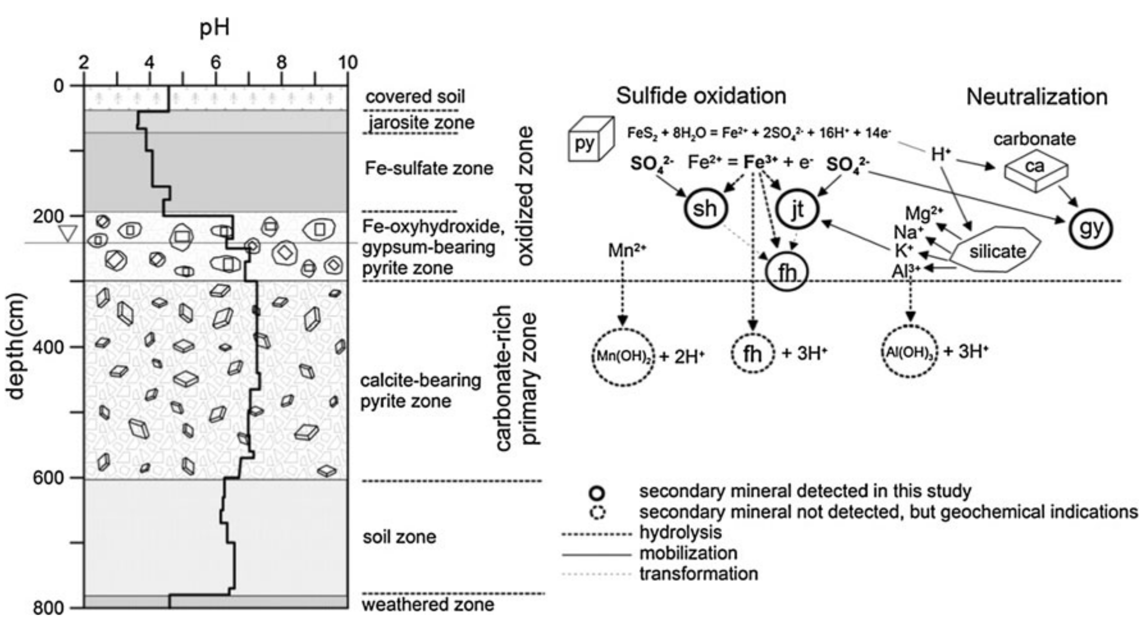


**Fig. 5** The proposed conceptual model of physico-chemical conditions and phases–water relationships controlling the element behaviors in the Guyrong mine tailings (Moon et al. 2008b). *fh* ferrihydrite, *jt* jarosite, *sh* schwertmannite, *gy* gypsum, *ca* calcite, and *py* pyrite

**Table 2** Principal component analysis (PCA) results using factors of 12-hole profile samples

| | PC1 | PC2 | PC3 | PC4 |
|---|---|---|---|---|
| Eigenvalue | 4.1 | 3.4 | 2.0 | 2.0 |
| % variance | 19.3 | 16.0 | 9.5 | 9.4 |
| Cumulative % | 19.3 | 35.3 | 44.7 | 54.2 |
| Variables | | | | |
| pH | 0.11376 | **0.68386** | 0.27556 | −0.31331 |
| CEC | **0.42598** | **−0.53072** | −0.20549 | 0.28137 |
| Clay | **0.94330** | −0.07598 | −0.07561 | 0.10008 |
| Silt | **0.93423** | 0.12949 | −0.05917 | −0.06232 |
| Sand | **−0.95517** | −0.09141 | 0.06364 | 0.03141 |
| Gypsum | −0.21997 | −0.24252 | 0.33106 | **0.44208** |
| Pyrite | −0.36955 | 0.09281 | 0.07891 | **−0.76479** |
| Jarosite | 0.09633 | −0.37158 | −0.07446 | **0.47822** |
| Calcite | 0.29463 | **0.68068** | −0.17395 | −0.10944 |
| Quartz | 0.23405 | **−0.68673** | −0.16779 | 0.31638 |
| Albite | **−0.48282** | −0.13980 | −0.01291 | **0.65695** |
| Chlorite | 0.25774 | **0.87528** | 0.10877 | −0.03113 |
| Mica | **0.59853** | **0.58943** | 0.01678 | 0.10072 |
| Orthoclase | 0.31351 | **−0.44923** | −0.12189 | −0.01964 |
| Fe | −0.11707 | 0.03556 | **0.85859** | 0.01046 |
| Mn | −0.03148 | 0.27301 | **0.82848** | −0.10682 |
| Al | −0.16796 | −0.08181 | −0.27085 | 0.18550 |
| Cu | 0.11311 | −0.06614 | −0.11428 | −0.22763 |
| Pb | 0.17657 | 0.05360 | −0.04133 | −0.35301 |
| Zn | −0.03918 | −0.00977 | 0.36870 | −0.01869 |
| Cd | 0.09359 | −0.07477 | −0.01889 | 0.00371 |

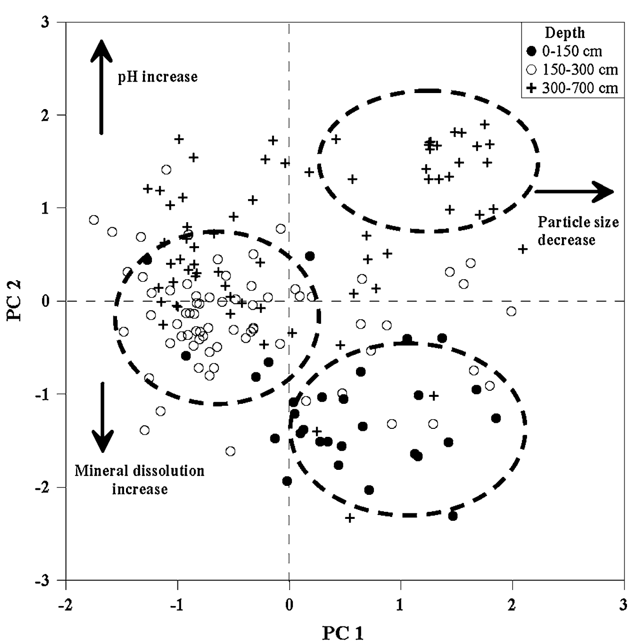


**Fig. 6** Plots of PC1 versus PC2 using physico-chemical–mineralogical analysis results for the 12 profiles

**Table 3** Average values of variants for each zone after cluster analysis for the 12-hole profile samples

| Variable | Cluster | | | | |
|---|---|---|---|---|---|
| | I | II | III | IV | V |
| pH | 3.72 | 3.65 | 4.97 | 5.49 | 7.00 |
| CEC | 12.43 | 5.42 | 2.25 | 2.17 | 3.61 |
| Clay | 13.85 | 6.81 | 4.46 | 5.57 | 13.63 |
| Jarosite | 1.86 | 2.25 | 0.09 | 0.19 | 0.00 |
| Gypsum | 1.95 | 9.95 | 4.21 | 7.73 | 0.39 |
| Pyrite | 0.06 | 7.89 | 43.66 | 23.09 | 14.11 |
| Calcite | 0.00 | 0.00 | 0.63 | 0.93 | 6.41 |
| Quartz | 62.99 | 34.17 | 19.36 | 22.66 | 18.95 |
| Albite | 11.47 | 20.70 | 9.33 | 13.62 | 6.50 |
| Chlorite | 9.65 | 12.86 | 16.04 | 23.08 | 39.20 |
| Mica | 3.89 | 4.19 | 4.10 | 5.68 | 10.66 |
| Orthoclase | 7.74 | 6.72 | 2.57 | 3.13 | 3.80 |
| Fe | 0.0361 | 0.1543 | 0.1691 | 0.2056 | 0.1352 |
| Mn | 0.0069 | 0.0062 | 0.0190 | 0.0326 | 0.0249 |

largest absolute correlation among each variable and any cluster function. The groups for the CA were discriminated by their location within the tailings. Group I had the greatest CEC, and group II had the smallest pH condition and the greatest jarosite and gypsum content. Groups III and IV differed by their particle size distributions. The calcite identified in group V had a neutral pH. Ultimately, the pH and minerals can be interpreted as the most significant variables in the cluster analysis.

3D-coupled Markov chain modeling

A brief description of the CMC (Elfeki and Dekking 2001), modeling described it as stochastic in nature. The CMC, coupled Markov chains, the first of which was used to describe the sequence of lithologies in the vertical direction and the second in the horizontal direction (Elfeki 2006). The CMC modeling has great potential to be integrated with soft information such as geological inference and geophysical data because of its explicit scheme. The applications of CMC on outcrops and real borehole data are available (Elfeki and Dekking 2005; Elfeki 2006). The surface and subsurface heterogeneities are complex mixtures of discrete structures, which may be categorized by soil type or geology and are characterized by more or less discontinuous boundaries and random features (Park et al. 2007). For the spatial distribution of the tailings, the 3D-CMC simulation technique is applied for revealing the distribution of each horizon. The 3D-CMC modeling was applied to the cross section in Fig. 1 (60 × 40 × 7 m). Figure 7a is simulated solely from the realized result using five zonations from the 12-hole cluster analysis. The

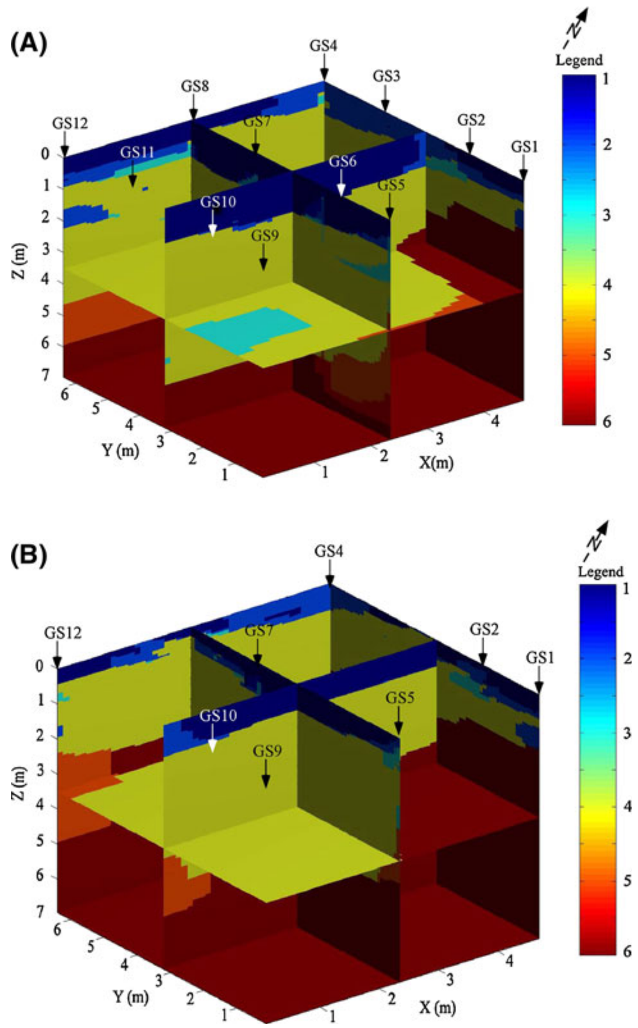


**Fig. 7** 3D-CMC simulated singly realization result using zonation for the 12 holes (**a**) and the 8 holes (**b**) from cluster analysis result

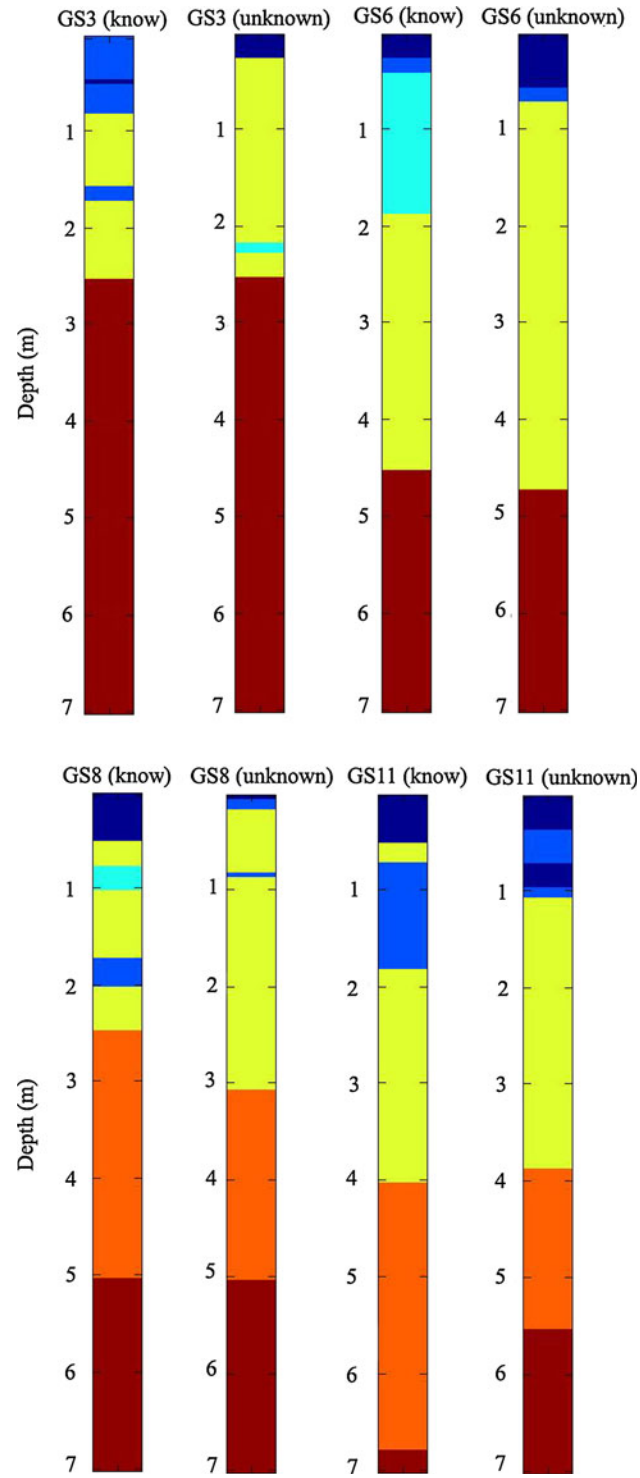


**Fig. 8** Compared GS3, GS6, GS8 and GS11 profiles (known) for 12 holes with GS3, GS6, GS8 and GS11 profiles (unknown) predicted for 8 holes data by 3D-CMC modeling. The 8 holes excluded GS3-, 6-, 8- and 11-hole data

detailed soil logging of 12 boreholes within a relatively small area is available. In each borehole, the soil is sample at every 0.05-m interval. The model domain was divided into 434,700 cells with dimension of 1 × 1 × 0.05 m. Group VI not including the tailing is bottom soil. The tailings were buried deeper into the southwest. For the cost-saving prediction of subsurface heterogeneity, 3D-CMC modeling was, respectively, performed on the 6-profile, the 8-profile and the 10-profile data among 12-profile data. The predicted groups were classified correctly 75.3 % (6 profiles), 85.0 % (8 profiles) and 96.3 % (10 profiles), respectively. The 8 profiles were calculated as the most efficient profile number (Fig. 7b). To identify the 3D distribution of subsurface heterogeneity, the 3D-CMC modeling required borehole data of the angular points and those within 40 m in this study area. The result of the unknown four holes as CMC modeling is comparable to the known hole data (Fig. 8). The unknown four holes, GS3, GS6, GS8 and GS11, are identified as 89.1, 88.6, 80.7 and 81.1 %, respectively (Table 4). The 3D-CMC modeling can be applied to the 3D distribution of subsurface

**Table 4** Prediction results discriminant analysis and CMC modeling for the GS3, GS6, GS8 and GS11 holes

| Methods | Correct index of predicted group | | | | |
|---|---|---|---|---|---|
| | GS3 | GS6 | GS8 | GS11 | Total |
| CMC modeling (%) | 89.72 | 88.59 | 80.72 | 81.13 | 85.04 |

heterogeneity and used in the characterization of the surface environment.

## Conclusions

The detailed vertical and horizontal distribution of the site was crucial to design an efficient risk management system associated with the tailings from abandoned mines. The detailed characterization of mineralogical alteration with depth and of the risks associated with rich pyrite tailings from abandoned mine provides insight into the future of the geochemical progression of the tailings. Various physicochemical and mineralogical results could be simplified using the PCA, which was applied to determine the interrelations among the 21 variables examined in the tailings. The factor analysis indicates that tailing composition, which accounts for 54.2 % of the total variance of 21 variables, is mainly affected by three factors: pH, particle size and mineral composition. In addition, the cluster analysis was employed for the vertical zonation of the tailings. The groups for the cluster analysis were divided into five zones that altogether captured the entire profile of the Guyroung mine tailings. In groups I and II, the presence of jarosite and gypsum was confirmed by the oxidation of pyrite. Groups III and IV differ from the other groups in their particle size. Group V was identified as having calcite ($CaCO_3$) and a neutral pH. These results were compiled in a database, and by applying the CMC, the quantitative 3D distribution of the tailings was confirmed. The mineralogical and geochemical changes were investigated among the zones in sulfuric copper tailings. The different depths in the same zone can enable the prediction of the oxidation processes occurring in the sulfide minerals. For the cost-saving prediction of subsurface heterogeneity, 3D-coupled Markov chain (3D-CMC) modeling was, respectively, performed on the 6 profile, the 8 profile and the 10 profile data among 12 profiles data. The 8 profile is calculated as the most efficient profile number. The profiles predicted by 3D-CMC modeling unknown holes (GS3, GS6, GS8, and GS11) are identified as 89.1, 88.6, 80.7 and 81.1 %, respectively. These can be applied to design an efficient method of managing from abandoned mines.

**Acknowledgments** This research was conducted as a part of the Core Environmental Technology Development Project for Next Generation (Eco-Technopia 21) of the Korean Institute of Environmental Science and Technology (KIEST) under contract 04003-0008 and the Overall management of Korea farmland for green country formation Project of Rural Development Agricultural (RDA) under contract 11-29-69.

## References

Acosta JA, Faz A, Martinez-Martinez S, Zornoza R, Carmona DM, Kabas S (2011) Multivariate statistical and GIS-based approach to evaluate heavy metals behavior in mine sites for future reclamation. J Geochem Explor 108:8–17

Anderberg MR (1973) Cluster analysis for applications. Academic Press, New York

Blowes DW, Jambor JL (1990) The pore-water geochemistry and the mineralogy of the vadose zone of sulfide tailings, Waite Amulet, Quebec, Canada. Appl Geochem 5:327–346

Blowes DW, Jambor JL, Hanton-Fong CJ (1998) Geochemical, mineralogical and microbiological characterization of a sulphide-bearing carbonate-rich gold-mine tailings impoundment, Joutel, Quebec. Appl Geochem 13:687–750

Borden D, Giese RF (2001) Baseline studies of the clay minerals society source clays: cation exchange capacity measurements by the ammonia-electrode method. Clay Clay Miner 49:444–445

Carle SF, Fogg GE (1996) Transition probability-based indicator geostatistics. Math Geol 28:453–476

Carle SF, Fogg GE (1997) Modeling spatial variability with one and multidimensional continuous Markov chains. Math Geol 29:891–917

Davis JC (1986) Statistics and data analysis in geology. Wiley, New York

Elfeki AMM (2006) Reducing concentration uncertainty using the coupled Markov chain approach. J Hydrol 317:1–16

Elfeki AMM, Dekking MA (2001) Markov chain model for subsurface characterization: theory and applications. Math Geol 33:569–589

Elfeki AMM, Dekking M (2005) Modeling subsurface heterogeneity by coupled Markov chains: directional dependency, Walther's law and entropy. Geol Geotech Eng 23:721–756

Gauch HG (1993) Prediction, parsimony, and noise. Am Sci 81:468–478

Grande JA, Gonzalez A, Beltran R, Sanchez-Rodas D (1996) Application of factor analysis to the study of contamination in the aquifer system of Ayamonte-Huelva (Spain). Ground Water 34:155–161

Häkli TA (1970) Factor analysis of the sulphide phase in mafic and ultramafic rocks in Finland. Bull Geol Soc Finland 42:109–118

Hwang CK, Cha JM, Kim KW, Lee HK (2001) Application of multivariate statistical analysis and a geographic information system to trace element contamination in the Chungnam Coal Mine area, Korea. Appl Geochem 16:1455–1464

Joliffe IT (1986) Principal component analysis. Springer, New York

Kaiser HF (1958) The varimax criterion for analytic rotation in factor analysis. Psychometrica 23:187–200

Kim WJ, Oh IS (1966) Investigation report on the Guyong Copper and pyrite mine. Geol Surv Korea 9:198–216

Kim J-H, Kim R-H, Lee J, Cheong T-J, Yum B-W (2005) Multivariate statistical analysis to identify the major factors governing groundwater quality in the coastal area of Kimje, South Korea. Hydrol Process 19:1261–1276

Lambrakis N, Antonakos A, Panagopoulos G (2004) The use of multicomponent statistical analysis in hydrogeological environmental research. Water Res 38:1862–1872

Langmuir D (1997) Aqueous environmental geochemistry. Prentice Hall, New Jersey

Li W (2006) Transiogram: a spatial relationship measure for catergorical data. Int J Geogr Inf Sci 20:693–699

Li W, Zhang C (2005) Application of transiograms to Makov chain simulation and spatial uncertainty assessment of land-cover classes. GISci Remote Sens 42:297–319

McGregor RG, Blowes DW, Jambor JL, Robertson WD (1998) The solid-phase controls on the mobility of heavy metals at the Copper Cliff tailings area, Sudbury, Ontario, Canada. J Contam Hydrol 33:247–271

Min JS, Jung YW, Lee HJ, Lee ST, Na HJ, Chun CH (1998) Study on the environmental and safety problems and their remediation around mining areas. KIGAM Research Report KR-98(C)-48, pp 55–81

Moon Y (2007) Prediction of heavy metal behaviors and factor controlling oxidation of tailings in an abandoned mine. Ph.D. Dissertation, Yonsei University, Seoul, Korea

Moon Y, Kim J-Y, Song Y, Moon H-S (2008a) Physico-chemical and mineralogical characterization of the tailings in the Guryoung mining area. Econ Environ Geol 41:183–199

Moon Y, Song Y, Moon H-S (2008b) The potential acid-producing capacity and factors controlling oxidation tailings in the Guryong mine, Korea. Environ Geol 53:1787–1797

Nordstrom DK (1982) Aqueous pyrite oxidation and the consequent formation of secondary minerals. In Acid Sulphate weathering Soil Sci Soc Am pp. 37–56

Park E (2010) A multidimensional, generalized coupled Markov chain model for surface and subsurface characterization. Water Resour Res 46:W11509. doi:10.1029/2009WR008355

Park E, Elfeki AMM, Dekking FM (2005) Characterization of subsurface heterogeneity: integration of soft and hard information using multi-dimensional Coupled Markov chain approach. Dev Water Sci 52:193–202

Park E, Elfeki AMM, Song Y, Kim Y (2007) Generalized Coupled Markov chain model for characterizing categorical variables in soil mapping. Soil Sci Soc Am J 71:909–917

Ross S (2000) Introduction to probability models, 7th edn. Academic Press, San Diego

Saager R, Esselaar PA (1969) Factor analysis of geochemical data from the Basal Reef, Orange Free State, Goldfield, S. Africa. Econ Geol 64:445–451

SPSS (2001) SPSS base 12.0 User's Guide

Taylor JC, Zhu R (1992) Simultaneous use of observed and calculated standard profiles in quantitative XRD analysis of minerals by the multiphase Rietveld method: the determination of pseudorutile in mineral sands products. Powder Diffr 7:152–161

Wold S (1987) Principal component analysis. Chemomet Intell Lab Syst 2:17–52